

CENTRAL COLLISIONS BETWEEN HEAVY NUCLEI AT  
EXTREMELY HIGH ENERGIES: THE FRAGMENTATION REGION\*

R. Anishetty<sup>†</sup>  
Physics Department  
University of Washington, Seattle, Washington 98195

P. Koehler and L. McLerran<sup>‡</sup>  
Stanford Linear Accelerator Center  
Stanford University, Stanford, California 94305

ABSTRACT

We discuss central collisions between heavy nuclei of equal baryon number at extremely high energies. We make a crude estimation of the energy deposited in the fragmentation regions of the nuclei. We argue that the fragmentation region fragments thermalize, and two hot fireballs are formed. These fireballs would have rapidities close to the rapidities of the original nuclei. We discuss the possible formation of hot, dense quark plasmas in the fireballs.

Submitted to Physical Review D

---

\* Work supported by the Department of Energy under contract numbers DE-AC03-76SF00515 (SLAC) and DE-AC06-76ER01388 (Washington).

† Address after September 1, 1980: Physics Department, Brandeis University, Waltham, Massachusetts 02154.

‡ Address after September 15, 1980: Physics Department, University of Washington, Seattle, Washington 98195.

## 1. Introduction

The collisions of very high energy nuclei are likely to be the subject of intense experimental investigation in the next few years. For high energy cosmic rays, the spectrum of primary cosmic rays with energies  $E > 10$  TeV is widely believed to be composed largely of nuclei such as Fe.<sup>1-4</sup> This beam of high energy nuclei may be employed in high altitude balloon emulsion chamber experiments, in experiments proposed for the space-lab, or in the Fly's Eye experiment.<sup>5-8</sup> The next generation of heavy ion accelerators may also allow for high statistics experimental studies of these collisions.<sup>9-12</sup> In particular, the Venus accelerator may ultimately achieve center of mass energies of 30 GeV/nucleon in collisions of uranium nuclei.

We shall discuss theory of such collisions in this paper. We shall concentrate on describing central collisions between nuclei of equal baryon number. These collisions comprise a considerable proportion of high energy nucleus-nucleus collisions. For a uranium nucleus,  $R \sim 7.4$  fm, geometrical considerations suggest that collisions with impact parameters  $b \lesssim 1$  fm are  $\sim \frac{1}{2}\%$  of the total. The high multiplicities of these central collisions provide an unmistakable signal of their occurrence. These multiplicities are so large,  $\langle n \rangle \gtrsim 10^3 - 10^4$ , that only extremely rare statistical fluctuations in the multiplicities generated by peripheral collisions will simulate a central collision.

The fragmentation regions of the nuclei represent an area of phase space where new phenomena might occur. "Fragmentation region" refers to the region of phase space of particles where the particles have longitudinal momentum close to that of the original nucleus projectile or

target. In the fragmentation region, the nucleus fragments and inelastically produced particles might form a hot, dense fireball. We shall soon see that this formation appears probable.

In such a hot, dense fireball, we might find evidence for the production of a quark plasma. The existence of a quark plasma in the early universe, and its possible production in the cores of heavy neutron stars, has been extensively discussed.<sup>12-37</sup> Attempts have also been made to analyze possible production mechanisms in intermediate energy nucleus-nucleus collisions.<sup>38-41</sup> The corresponding problem for very high energy nucleus-nucleus collisions has not been fully addressed, although considerable effort has been carried out to simulate nucleus-nucleus collisions as observed in cosmic ray experiments.<sup>42-43</sup>

High energy nucleus-nucleus collisions are actually simple to analyze. At high energies, hadron-nucleus data indicate that nuclei are "transparent".<sup>44-53</sup> In such collisions the projectile hadron and its fast fragments are distributed almost as if the hadron had undergone a collision with only one other hadron. The distribution of the slow fragments, depends, of course, on the thickness of the nuclear target. The phase space distribution of the projectile and fast fragments in this hadron-nucleus collision is fairly well approximated by the corresponding distributions for hadron-hadron scattering.

This fact is at first glance surprising. In a collision of a hadron with a heavy nucleus, the hadron must penetrate several mean free paths of nuclear matter. We might expect, therefore, that the hadron and its fragments would undergo multiple scatterings and a shower would develop.

The 'absence of such shower formation is however, simple to understand.<sup>54-63</sup> The hadron's fast fragments are produced outside the nucleus. There is insufficient time for the production of these fast fragments while the hadron traverses the nucleus. We shall study this production in detail in the next sections.

Elastic collisions and the production of slow fragments only slightly modify the phase space distribution of the hadron and its fast fragments. Since these modifications involve very little energy transfer, the hadron projectile traverses the nucleus at the velocity of light, and does not slow down significantly while passing through the nucleus. The matter distribution of the target has little time to adjust to the presence of this fast projectile, and an impulse approximation should be valid.

The situation should be correspondingly simple in nucleus-nucleus collisions.<sup>62</sup> In these collisions the projectile nucleus may be viewed as a Lorentz contracted pancake which passes through the target nucleus at the velocity of light. This projectile nucleus does not fragment until it has passed through the target, and does not slow down significantly while passing through. The constituents of the pancake projectile may be expected to almost behave as if they scattered inelastically once in traversing the nucleus.

The distribution of these projectile nucleus fragments is not, however, the same as the distribution in hadron-nucleus scattering. The fast projectile fragments rescatter off one another before emerging from the pancake.

We may understand this rescattering from a different vantage point by studying the target fragments. The target fragments are produced as

the Lorentz contracted projectile passes through the target. At very high energies this projectile has a limiting thickness of  $r \lesssim R_0 \sim 1 \text{ fm}$ .<sup>62</sup> The target constituents scatter inelastically only once off the projectile, since the thin projectile passes through a nucleon constituent before the target constituent has time to fragment. Shortly after the passage of the projectile nucleus through the target constituent, that constituent fragments. The fragments produced should have a phase space distribution which is typical of hadron-hadron inclusive scattering. These fragments are, however, produced in the nuclear matter and in the presence of many other constituent target fragments. Many rescatterings will occur before the fragments emerge from the target.

If the nuclei are large enough, and if the expansion rate of the nucleus is slow enough, the nucleus fragments will equipartition their energies by rescattering. We shall soon see that it is indeed probable that this does occur. If such thermalization occurs, a hot plasma of hadronic matter would be formed. If the plasma is hot and dense enough, a plasma of quarks and gluons would result. These quarks and gluons would very probably be freed from their nucleons in the initial nucleus-nucleus collision. Under ordinary circumstances, these quarks and gluons would quickly recombine into hadrons. In this extraordinarily hot, dense environment, they might however remain in a plasma phase. We shall estimate that in high energy nucleus-nucleus collisions, the hadronic matter is just hot and dense enough that a quark-gluon plasma might be formed.

In the head-on nucleus-nucleus collisions which we are discussing, two fireballs are formed, one in each of the fragmentation regions of the

nuclei.<sup>64-65</sup> We do not address the problem of understanding the hot, dense mesonic matter which is formed in the central region of rapidity. This mesonic matter presumably forms a hot fire-tube which joins the nucleus fragmentation regions.<sup>66</sup> The formation and dynamics of this fire-tube should be a subject of further study.

An ideal situation for studying these fireballs would be in a colliding-nucleus facility. Correlations between the energies and decay products of the fireballs could be studied on an event-by-event basis to select central collisions. Another method well tailored to experimental exploration of these collisions would employ emulsions in high altitude cosmic ray experiments. High multiplicity nuclear fragmentations are directly accessible in emulsion.<sup>5,8</sup> Selecting those events which are highest in multiplicity could easily be accomplished by visual scanning. Finally, the Fly's Eye experiment may access the highest energy component of cosmic rays.<sup>6</sup> The calorimetry information gathered by measuring the longitudinal development of the cosmic ray showers, and the information gleaned from the proposed muon arrays may allow for a unique study of nucleus fragmentations as high energy cosmic ray nuclei interact with air nuclei at the top of the atmosphere.

We shall develop here the theoretical description of the process of formation of the nuclear fireballs, describing the formation and initial evolution of the plasma in terms of nucleons and mesons. The dynamics of a quark-gluon plasma will be analyzed in a later paper. We shall here concentrate on developing a physical, intuitive picture of fireball formation, and attempt to estimate the order of magnitude of the energy density, quantum numbers, size, and lifetime of the plasma. We shall

investigate the self-consistency of a thermodynamic description of the fireballs.

The organization of this paper is as follows: in the next section, we review the space-time description of hadron-hadron and hadron-nucleus scattering offered by Gottfried, Bjorken, and others.<sup>54-63</sup> We discuss implications of this description for nucleus-nucleus scattering. We argue that the energy deposited in the nucleus fragmentation regions may be crudely estimated from the experimentally measured proton-proton inclusive fragmentation functions. Using the data of Thomé et al., and Capiluppi et al., we obtain crude parameterizations of these fragmentation functions.<sup>67-68</sup>

In the third section, we discuss criteria which must be satisfied by inelastically produced particles and scattered nucleons, if such particles are to be trapped in the nucleus fragmentation regions. We employ these criteria to estimate the energy per nucleon, energy density, density, quantum numbers and total momentum of the fireball.

In the fourth section, we discuss the thermodynamics of the produced fireballs. We argue that the mean free path of hadrons is small enough, and the cooling time is long enough so that the constituents of a fireball produced in a head-on uranium nucleus-uranium nucleus collision will come into thermodynamic equilibrium. We argue that the fireballs are hot and dense enough that a quark-gluon plasma may be formed. We discuss problems associated with large thermal gradients in the produced fireballs.

## 2. Hadron-Hadron and Hadron-Nucleus Collisions

The description of high energy nucleus-nucleus collisions which we shall offer rests on the theoretical foundations of high energy hadron-hadron and hadron-nucleus collisions. We shall attempt to erect a description of the fragmentation regions of nucleus-nucleus collisions upon these foundations.<sup>54-63,69-73</sup> The nucleus fragmentation regions refer to those regions of phase space of particles where the particles' momenta are close to the momenta of either the projectile nucleus or target nucleus. The region of phase space where momentum is intermediate between the projectile and target is the central region.

The projectile and target fragmentation regions include the regions of phase space where many of the particles have quantum numbers of the constituents of the nucleus. In this region, there are also inelastically produced mesons. The central region, on the other hand, includes few projectile or target fragments, and consists primarily of mesons.

The close similarity between projectile and fast projectile fragment distributions in hadron-nucleus and hadron-hadron scattering is at first sight surprising. Nuclei are large, and a hadron fragment has several chances to rescatter before emerging from the nucleus.

Nuclear radii are well approximated by the formula

$$R(A) \cong 1.2A^{1/3} \text{ fm} \quad . \quad (2.1)$$

where A is the baryon number of the nucleus. A few typical nuclear radii are displayed in Table 1. The mean free path of a high energy proton is much smaller than the radius of a heavy nucleus such as Pb or U. Using a proton-proton cross section of

$$\sigma_{\text{tot}}^{\text{pp}} = 40 \text{ mb} \quad , \quad (2.2)$$

and nuclear matter density of

$$\mathcal{N}_{\text{nuc}} = \frac{A}{4/3 \pi R^3(A)} \approx .15 \text{ baryons/fm}^3 \quad (2.3)$$

the nucleon mean free path is

$$\lambda_{\text{nuc}} \approx 1.6 \text{ fm} \quad (2.4)$$

The reason that the distribution of projectile and fast projectile fragments is quite similar in hadron-hadron and hadron-nucleus collisions is simple. The hadron projectile changes its energy only slightly when it undergoes an elastic scattering or emits a low energy fragment. These processes can occur while the hadron traverses a nucleus. The fast fragments associated with inelastic scattering, however, do not form until after the hadron has traversed the nucleus. In the rest frame of the hadron projectile, the characteristic time for emission of these fragments is the time it takes light to fly a Fermi,  $\tau \sim R_0$ . In the rest frame of the target nucleus, on the other hand,

$$\tau \sim \frac{E}{M} R_0 \quad (2.5)$$

where  $E$  is the projectile energy and  $M$  is the projectile mass. These fragments are emitted with a distribution characteristic of an inelastically scattered proton, a distribution which is approximately independent of the excitation process. We should note, however, that the ratio of the sum of the elastic and diffractive dissociation cross sections to the inelastic cross section should be quite small for a hadron which passes through the nucleus. Since the hadron has several opportunities to scatter inelastically, it will almost certainly take advantage of one of them.

These properties of high energy hadron-nucleus scattering greatly facilitate the analysis of nucleus-nucleus scattering. For the sake of simplicity, we shall consider only head-on collisions between nuclei of equal baryon number. In such a head-on collision, a constituent of the projectile nucleus travels many mean free paths before passing through the target nucleus. This constituent should scatter inelastically at least once while passing through the target. Since subsequent inelastic scatterings of the projectile constituent with the target nucleons will not greatly change the phase space distribution of projectile fragments, we conclude that the projectile nucleon fragments are almost distributed as if the projectile had scattered only once.

If we could ignore the rescattering of projectile fragments with one another, then the phase space distribution of projectile fragments would be directly determined from high energy proton-proton scattering. These rescattering effects are of course crucial in the formation of a plasma. We have argued, however, that this plasma formation occurs after the nuclei pass through one another. The phase space distribution of produced fragments which rescatter to form the plasma should be determined from pp inclusive scattering data. The rescattering of fragments and plasma formation are the subjects of the next sections.

The distribution functions for inclusive production of hadrons in  $pp \rightarrow hX$  approximately scale. In terms of center-of-mass longitudinal momentum fraction,  $x$ , and transverse momentum,  $p_{\perp}$ , the differential inclusive cross sections are fit well by the factorized form<sup>69-72</sup>

$$E_h \frac{d^3\sigma_h}{d^3p} = F_h(x) g_h(p_{\perp}) \quad . \quad (2.6)$$

These structure functions are normalized to

$$\int d^3p \frac{d^3\sigma_h}{d^3p} = \langle n_h \rangle \sigma_{inel}^{tot} \quad (2.7)$$

where  $\sigma_{inel}^{tot} \sim 32$  mb is the total inelastic pp cross section and  $\langle n_h \rangle$  is the multiplicity of hadrons of species h.

In the analysis of the next section, we shall use the structure functions of Eq. (2.6) as determined from a fit to the data of Capiluppi et al.<sup>68</sup> We shall present the details of our fit to these data in the remainder of this section. We must make two comments about our fit. First, our fit is accurate to only 10-20%. Such a fit is sufficiently accurate for the conclusions we draw in later sections, but is not a precise fit derived from a comprehensive data analysis. We have not carried out any statistical analysis of our fit. Second, we have modified the form of Eq. (2.6) by allowing  $F_h(x)$  to have a slight energy dependence. Our fit with this energy dependence is only valid in the energy range of 30-70 GeV. In other energy ranges, our parameterization must surely be modified if for no other reason than to maintain momentum sum rules. Our parameterizations satisfy these sum rules to an accuracy of 15% in the energy range of 30-70 GeV.

We parameterize the  $p_{\perp}$  dependence of  $g_h(p_{\perp})$  in Eq. (2.6) as

$$g_h(p_{\perp}) = e^{-\lambda_h p_{\perp}} \quad (2.8)$$

Our fit to the Capiluppi data is

$$\begin{aligned} \lambda_{\pi^+} &= \lambda_{\pi^-} \cong 5.1 \text{ GeV}^{-1} \\ \lambda_{K^+} &= \lambda_{K^-} \cong 4.2 \text{ GeV}^{-1} \end{aligned} \quad (2.9)$$

and

$$\lambda_p \cong 3.8 \text{ GeV}^{-1} \quad . \quad (2.10)$$

The rise in the height of the central plateau, and the consequent energy dependent modification of Eq. (2.6) is obtained from the data of Thomé et al.<sup>67</sup> Their data on  $\left. \frac{d\sigma}{dy} \right|_{y=0}$  are fit by

$$\left. \frac{d\sigma}{dy} \right|_{y=0} = (22 \ln E_{\text{c.m.}} - 28) \text{ mb} \quad . \quad (2.11)$$

The parameter  $y$  in this equation is the center-of-mass rapidity. The fit of this equation is valid for  $30 \text{ GeV} < E_{\text{c.m.}} < 63 \text{ GeV}$ .

In this central region, the inelastically produced particles are primarily pions. There is a small  $\sim 10\%$  contamination of kaons. Allowing for this contamination by requiring that our formulae for the  $x$  and  $p_{\perp}$  distributions of pions and kaons integrate to the correct multiplicity at  $E \approx 50 \text{ GeV}$ , we have found that

$$F_{\pi^+}(0) \cong F_{\pi^-}(0) \cong (40 \ln E - 50) \text{ mb/GeV}^2 \quad . \quad (2.12)$$

The  $pp \rightarrow \pi^{\pm}X$  data were fit to the forms

$$F_{\pi^+}(x) = (F_{\pi^+}(0) - \alpha_{\pi^+})(1-x)^7 + \alpha_{\pi^+}(1-x)^3 \quad (2.13)$$

and

$$F_{\pi^-}(x) = (F_{\pi^-}(0) - \alpha_{\pi^-})(1-x)^7 + \alpha_{\pi^-}(1-x)^4 \quad . \quad (2.14)$$

The coefficients  $\alpha_{\pi^{\pm}}$  were chosen to be energy independent. The energy dependent factors of  $F_{\pi^{\pm}}(0)$  were chosen to multiply  $(1-x)^7$ , since these terms are important at small  $x$  where scaling violation is observed. The powers of  $(1-x)$  in Eqs. (2.13)-(2.14) are chosen to be consistent with

quark counting rules.<sup>74-75</sup> Our fit to the data of Capiluppi et al. is<sup>68</sup>

$$F_{\pi^+}(x) = (40 \ln E - 139)(1-x)^7 + 89(1-x)^3 \text{ mb/GeV}^2, \quad (2.15)$$

and

$$F_{\pi^-}(x) = (40 \ln E - 91)(1-x)^7 + 41(1-x)^4 \text{ mb/GeV}^2. \quad (2.16)$$

The  $K^+$ ,  $K^-$  inclusive data is well fit by

$$F_{K^+}(x) = .1 F_{\pi^+}(x), \quad (2.17)$$

and

$$F_{K^-}(x) = .1 F_{\pi^+}(0)(1-x)^7. \quad (2.18)$$

The form of Eq. (2.17) is suggested by the fact that the  $K^+$  and  $\pi^+$  both arise from the same valence quarks of the protons and the form of Eq. (2.18) by the fact that all the  $K^-$  quarks arise from the sea of quark-antiquark pairs.

The distribution of neutral pions and kaons was not determined by Capiluppi et al.<sup>68</sup> The quark model and data on  $\pi^0$  multiplicities suggest a simple parameterization for the neutral pion and kaon distributions. Since the  $\pi^0$  is composed of equal components of  $u\bar{u}$  and  $d\bar{d}$  quarks, we expect that

$$F_{\pi^0}(x) \approx \frac{1}{2} (F_{\pi^+}(x) + F_{\pi^-}(x)). \quad (2.19)$$

This formula has the correct limiting behavior near  $x=0$ , where distributions should be isospin symmetric.

The  $K^0$  is composed of  $d\bar{s}$  quarks and the  $\bar{K}^0$  is composed of  $\bar{d}s$ , so that

$$F_{K^0}(x) = .1 F_{\pi^-}(x), \quad (2.20)$$

and

$$F_{\bar{K}^0}(x) = .1 F_{\pi^-}(0)(1-x)^7 \quad (2.21)$$

are suggested by analogy with Eqs. (2.17) and (2.18).

The determination of the baryon structure function is simplified by noting first that outside of a small region of  $x \sim 1$ , the proton structure function is proportional to  $x$ . For extremely small  $x$ , however, the proton structure function approaches a small constant value which corresponds to baryon-antibaryon pair production. These pairs contribute only a small amount to the multiplicity, and we shall ignore their effect.

The contribution to the structure function for  $x \sim 1$  corresponds to small angle diffractive dissociation, and contributes a significant amount,  $\sim 10$ - $20\%$  to the total baryon multiplicity. Since we are interested in applying these pp inclusive scattering data to central nucleus-nucleus collisions, however, this contribution should be negligible. The nucleons in a central nucleus-nucleus collision will probably scatter inelastically, without diffractive dissociation.

The structure function for inclusive baryon production, ignoring the complications mentioned above for  $x \approx 0$  or  $x \approx 1$ , is

$$F_B(x) = 74x \text{ mb/GeV}^2 \quad . \quad (2.22)$$

The coefficient of  $x$  in this equation is determined so that the sum rule of Eq. (2.7) is satisfied. Since  $\langle n_B \rangle = 2$ , this sum rule is

$$\int d^3 p \frac{d^3 \sigma}{d^3 p} = 2\sigma_{\text{inel}}^{\text{tot}} \quad . \quad (2.23)$$

These formulae for inclusive distributions can be integrated and the resulting numbers can be compared to the experimentally measured values for total charged particle multiplicities. The results of such a comparison are shown in Table 2. For  $30.8 < E_{\text{c.m.}} < 62.8$  GeV, our fit reproduces the data to an accuracy  $\sim 15\%$ .

### 3. The Fireballs

In this section, we discuss the formation of fireballs from the nucleus fragments of a nucleus-nucleus collision. We discuss criteria which the fragments must satisfy in order that they may thermalize and form a hot, dense hadronic plasma. We estimate the energy, momentum, and quantum numbers of these trapped particles.

In order that a fragment may thermalize and become ensnared by other fragments in the nucleus fragmentation regions, the fragment must scatter several times off other nucleus fragments. Data on hadron-nucleus scattering indicate, however, that fast fragments of a projectile hadron do not rescatter inelastically as they pass through the nucleus.

This lack of rescattering is a consequence of the inside-outside cascade development of the shower of inelastically produced particles. Only slow hadron fragments materialize inside the nucleus; the fast hadron fragments are produced outside the nucleus after the projectile has passed through the nucleus.

To understand this cascade mechanism a little better, consider the hadron fragmentation illustrated in the hadron-nucleus collision displayed in Fig. 1.<sup>62</sup> The inelastic fragment is produced with laboratory momentum of  $p_{\parallel}$ ,  $p_{\perp}$ . The fragment is produced in a collision at a distance  $r_{\parallel}$  from the exit point of the hadron projectile from the nucleus. The fragment propagates a distance of  $r_{\perp}$  from the projectile hadron while traversing the nucleus. Since most fragments are pions and therefore relativistic with  $v \approx 1$ , the projectile and projectile fragment separate only a small longitudinal distance while traversing the nucleus. Even in the case of kaons, most fragments are produced with large longitudinal momentum and

therefore have  $v \approx 1$ . The separation at the exit point of the hadron projectile from the nucleus is therefore

$$\Delta r \approx r_{\perp} \approx \frac{p_{\perp}}{p_{\parallel}} r_{\parallel} \quad (3.1)$$

A projectile and its fragment should separate a distance of a Fermi or greater before the fragment may rescatter. If the separation is less than a Fermi, the fragment would be included as a parton excitation of the projectile. This excitation is emitted from the projectile after the projectile has passed through the nucleus. Excitations are emitted with distributions almost typical of hadron-hadron scattering, a fact that is a consequence of the near-independence of the projectile excitation spectrum from the details of excitation dynamics.

In order for the fragment to be able to rescatter, therefore, the fragment should be produced with transverse momentum satisfying

$$p_{\perp} > \lambda p_{\parallel} \frac{R_0}{R} \quad (3.2)$$

where  $R_0 \sim 1$  fm,  $\lambda$  is a parameter of order one, and  $R$  is the nuclear radius.

If this inelastic projectile fragment is sufficiently energetic, it will penetrate through the nucleus and not become trapped with the nucleus fragments. Just as in the case for the projectile, the fragment is not slowed substantially within the nucleus if it is so energetic that most of its fast fragments are produced outside the nucleus.

A precise evaluation of the energy deposition of these fragments is a complicated problem in cascade theory. Fortunately, we do not need to invoke such complicated calculations. We can see that most fragments

which satisfy Eq. (3.2), that is, which are produced inside the nucleus, also become trapped in the nucleus. For a target nucleus at rest, one criterion which a fragment must satisfy to become trapped in the nucleus is that

$$p_{\parallel} \lesssim M \frac{R}{R_0} \quad (3.3)$$

where  $M$  is an effective fragment mass,  $R$  is the nuclear radius and  $R_0 \sim 1$  fm. This formula represents the requirement that in the rest frame of the nucleus, the fragment has enough time to emit its fragments.

We are, however, considering the case of a moving target nucleus. The collision of the two nuclei imparts longitudinal momentum to the target nucleus. The result of Eq. (3.3) is modified, since we must include the  $\gamma$  factor of the moving fireball,

$$p_{\parallel} \lesssim \left( \gamma + \sqrt{\gamma^2 - 1} \right) M \frac{R}{R_0} \quad (3.4)$$

where

$$\gamma = E_{\text{F.B.}} / M_{\text{F.B.}} \quad (3.5)$$

and  $E_{\text{F.B.}}$  and  $M_{\text{F.B.}}$  are the energy and mass of the fireball. We shall find in our later analysis that  $\gamma \sim 2$ . Since the average  $p_{\parallel}$  of most fragments is  $\sim 1-2$  GeV, and an appropriate effective fragment mass is  $\sim 300$  MeV, most of the fragments which satisfy Eq. (3.2) also automatically satisfy Eq. (3.4).

In the analysis which we have carried out, we have employed the constraints of both Eqs. (3.2) and (3.4). Specifically, we have used

$$p_{\parallel} \lesssim f_i \left( \gamma + \sqrt{\gamma^2 - 1} \right) M_i \frac{R}{R_0} \quad (3.6)$$

where  $f_i$  is a parameter of order one and  $M_i$  is 300 MeV for pions and

500 MeV for kaons. Note that the typical momentum cutoff for pions arising from Eq. (3.2) is  $p_{\parallel} \lesssim 2$  GeV.

Finally, in the collision between the nuclei, target nucleus nucleons acquire longitudinal momentum. As was the case for projectile fragments, if these nucleons are sufficiently energetic they will penetrate through the nucleus and leave the fragmentation region. Only those nucleons which satisfy Eq. (3.6) become part of the nucleus fragmentation region. For nucleons, we use  $M_{\perp} \sim 1$  GeV in Eq. (3.6).

We shall not repeat in detail our analysis of the energy deposition in the nucleus fragmentation regions. The outline of our calculation is as follows: we integrate the inclusive structure functions for nucleon, pion, and kaon production using the cuts of Eqs. (3.2) and (3.6). We specifically evaluate the numbers, longitudinal momentum, and energy of particles trapped in the nucleus fireball. The fireball mass, or rest frame energy of the fireball is determined from

$$M_{\text{F.B.}} = \sqrt{E_{\text{F.B.}}^2 - P_{\parallel \text{F.B.}}^2}, \quad (3.7)$$

since the net transverse momentum of the fireball should be small.

Sensitivity to the cuts of Eqs. (3.2) and (3.6) is evaluated by varying  $\lambda$  and  $f_{\perp}$  between 1/2 and 2. The results of such an evaluation for uranium is shown in Table 3.

As discussed previously, our results are insensitive to the parameters  $f_{\perp}$ . Most of the fragments of the projectile which are produced inside the target nucleus become trapped in the nucleus fragmentation region. The recoiling target nucleons are also almost always trapped, the fraction being typically  $\sim .95$ . These nucleons are relativistic and carry an average longitudinal momentum of  $p_{\parallel} \sim 2.3 \pm .7$  GeV/nucleon.

The uncertainty in this number as well as the uncertainties in all of our calculations are due primarily to uncertainties in the parameter  $\lambda$ .

The number of trapped pions is  $3.5 \pm 1.5$  pions/nucleon. The longitudinal momentum of these pions is  $1.2 \pm .7$  GeV/pion.

The number of trapped kaons is small,  $\sim .2 \pm .1$  kaons/nucleon. The longitudinal momentum of these kaons is  $p_{\parallel} \sim 2.2 \pm 1.1$  GeV/kaon. The reason these kaons carry large longitudinal momenta is that kaons more energetic than pions are trapped in the fireball, since the  $p_{\perp}$  falloff for kaons is less steep than the corresponding falloff for pions. Kaons of larger  $p_{\perp}$  and therefore large  $p_{\parallel}$  may be produced in the nucleus.

Finally, the rest frame energy/nucleon is  $\sim 3.8 \pm 1.2$  GeV. The fireball is relativistic with  $\gamma \sim 2.0 \pm .6$ .

In Table 4, we present results parallel to those in Table 3 for different center-of-mass collision energies. In the energy range of  $30 \text{ GeV/nucleon} \leq E_{\text{c.m.}} \leq 70 \text{ GeV/nucleon}$ , the fireball masses and numbers of trapped particles undergo only 20% changes. These small changes are obviously due to the approximate scaling of the proton fragmentation functions.

Finally, in Table 5, we offer parameters for various nuclear radii. The energy deposition varies almost linearly with the radius. For  $R \sim 4.4$  fm corresponding to iron, the energy deposition is  $\sim 2.8$  GeV/nucleon in the fireball rest frame. For  $R \sim 7.4$  fm corresponding to uranium, the value is  $\sim 3.5$  GeV/nucleon.

#### 4. Thermodynamics

In this section, we shall discuss the self-consistency of a thermodynamic analysis of the properties of a nuclear fireball. We shall estimate the relationship between the average energy densities and number densities for a fireball. We estimate the approximate energy density above which a quark-gluon description of the fireball dynamics may be appropriate. With these crude estimates, the mean free paths of various particles within the fireball will be estimated. The approximate number of collisions that various particles experience before substantial cooling takes place is also calculated.

The energy per baryon of a fireball produced in the central collision between two uranium nuclei has been estimated in the previous section to be  $E/N \sim 3.5$  GeV/nucleon. This energy per baryon corresponds to an energy density of

$$\mathcal{E} \cong 525 \text{ MeV/fm}^3 \quad (4.1)$$

where nuclear matter density is taken as  $\mathcal{N}_{\text{nuc}} \approx .15$  baryons/fm<sup>3</sup>.

This estimate of the energy density is clearly an underestimate. During the collision process, the target nucleus becomes compressed. To estimate this compression, we may assume that the projectile nucleus is infinitesimally thin and sweeps through the target nucleus at the velocity of light. As the projectile sweeps through the target, it scatters first on the target nucleons closest to the incident projectile nucleus beam. When the first target nucleon is encountered, this target nucleon acquires a longitudinal velocity  $v$  which is, on the average, the velocity of the target nucleus fireball. The second nucleon is struck by the projectile in the time it takes the projectile to fly the longitudinal distance

which separates the first and second nucleon. Since the projectile has velocity  $v \approx 1$ , the change in separation between the two nucleons is

$$\Delta x = (1-v) x \quad (4.2)$$

where  $x$  is the longitudinal separation of the nucleons.

The change in separation given by Eq. (4.2) is the change measured in the rest frame of the initial target nucleus. In the rest frame of the fireball,  $\Delta x \rightarrow \gamma \Delta x$ . The compression is

$$\frac{\Delta x}{x} = \gamma - \sqrt{\gamma^2 - 1} \quad (4.3)$$

For  $\gamma \sim 2$ , this compression increases the density by  $\sim 3.5$ . The energy density of this compressed fireball is

$$\mathcal{E} \sim 2 \text{ GeV/fm}^3 \quad (4.4)$$

In the rest frame of the fireball, the fireball has the geometry of an ellipsoid.

This energy density is comparable to the energy density inside a proton,

$$\mathcal{E}_p \cong \frac{1}{4/3 \pi r_p^3} \sim 500 \text{ MeV/fm}^3 \quad (4.5)$$

The proton r.m.s. charge radius  $r_p \sim .8 \text{ fm}$  is used in this formula. At this fantastic energy density, we might expect that individual hadrons would lose their identities and a hot, dense quark-gluon plasma would be formed. These quarks and gluons may no longer be identified as the constituents of individual hadrons.

If a transition takes place at this low density, interactions between quarks and gluons are almost certainly important in shaping the dynamics of the quark-gluon plasma. Only at a much higher density corresponding to a distance scale of  $r \sim 1 \text{ GeV}^{-1} \sim 1/5 \text{ fm}$  should quark and gluon interactions be small. At this distance, scaling sets in for deep inelastic scattering. Since the densities we consider here correspond to larger distance scales, the order of magnitude estimates which we present should be swallowed with a large grain of salt.

The energy density of Eq. (4.4) may be translated into a number density. Since this energy density is of the same order of magnitude as the energy density of a proton, the quarks which generate this energy density should have an average energy which is typical of quarks inside a proton. This energy is  $\sim 300 \text{ MeV}$ . The number of quarks/ $\text{fm}^3$  is therefore

$$\mathcal{N}_q \sim 7 \text{ quarks}/\text{fm}^3 \quad . \quad (4.6)$$

If we think of the quarks and antiquarks as mesons and baryons, we can estimate the average baryon and meson number densities. The energy of quark-antiquark pairs in mesons is

$$\mathcal{E}_m \sim 600 \mathcal{N}_m \text{ MeV}/\text{fm}^3 \quad (4.7)$$

where  $\mathcal{N}_m$  is the meson number density. A meson corresponds to a quark-antiquark pair with  $300 \text{ MeV}/\text{quark}$ . The energy density in baryons is

$$\mathcal{E}_B \sim \mathcal{N}_B M_p \quad (4.8)$$

where  $\mathcal{N}_B$  is the baryon number density and  $M_p$  is the proton mass. Adding Eqs. (4.7) and (4.8) to obtain the energy density of Eq. (4.1), we find

$$\mathcal{N}_m \approx 2 \text{ meson}/\text{fm}^3 \quad (4.9)$$

or

$$\mathcal{N}_m \simeq 3 \text{ mesons/baryon} \quad . \quad (4.10)$$

This number is of the same order as the number of mesons which we estimated were deposited in the fireball in the central collision.

The mean free path of a nucleon in this plasma is given by

$$\lambda_n = \frac{1}{\sigma_{nn}\mathcal{N}_n + \sigma_{nm}\mathcal{N}_m} \quad (4.11)$$

where  $\mathcal{N}_n$  and  $\mathcal{N}_m$  are the nucleon and meson number densities, and  $\sigma_{nn}$  and  $\sigma_{nm}$  are the nucleon-nucleon and nucleon-meson cross sections. Using  $\sigma_{nn} \sim 40$  mb, and  $\sigma_{nm} \sim 26$  mb, we obtain

$$\lambda_n \sim 1/7 \text{ fm} \quad . \quad (4.12)$$

A corresponding calculation for mesons gives

$$\lambda_m \sim 1/5 \text{ fm} \quad . \quad (4.13)$$

These mean free paths are much smaller than nuclear radii, and if hadrons do not dissolve into quarks, effects caused by finite nuclear size should be small.

For quarks, the additive quark model gives  $\sigma_{qn} \sim \frac{1}{3} \sigma_{nn}$  and  $\sigma_{qm} \sim \frac{1}{3} \sigma_{nm}$ .

The quark mean free path is

$$\lambda_q \sim 1/2 \text{ fm} \quad . \quad (4.14)$$

This mean free path is close to the mean free path of a proton in nuclear matter. Since even for uranium nuclei finite nuclear size effects yield non-negligible corrections to infinite nuclear matter calculations, these finite size effects may be important also for quark-gluon matter calculations.

The primary cooling mechanisms for the plasma are evaporation and expansion. The approximate cooling rate may be evaluated by making an analogy with the popping of a balloon. We are implicitly assuming the absence of large velocity gradients induced by the nucleus-nucleus collision in the rest frame of the fireball when we make this analogy. Since the deposition of energy in the fireball during the collision process is non-uniform, velocity gradients are certainly present. We have estimated the magnitude of these gradients and have found them to be small. A thorough analysis of these gradients should be carried out for an accurate estimate of the cooling rate.

When the surface of a balloon pops, the high density air molecules near the surface of the balloon rush out into the lower density surrounding air. The air molecules at the center of the balloon, however, maintain themselves at high density until a sound wave propagating inwards from the surface communicates the fact that the balloon has popped. The characteristic time for rarefaction is therefore the time it takes a sound wave to propagate a balloon radius.

For the situation at hand, the velocity of a sound wave in nuclear matter is  $v \lesssim 1/\sqrt{3}$  of the velocity of light, since quark matter calculations always approach an ideal gas equation of state

$$P = \frac{1}{3} \mathcal{E} \quad (4.15)$$

from below for large  $\mathcal{E}$ . The velocity of sound is

$$v^2 = \frac{dP}{d\mathcal{E}} \quad (4.16)$$

The characteristic time before expansion begins for the compressed nucleus is

$$\tau \sim 4 \text{ fm} \quad , \quad (4.17)$$

a result which agrees with a more detailed analysis based on hydrodynamic equations.<sup>41</sup>

After the compressed nucleus begins to expand, some time passes before the nucleus cools to an energy density of the order of the hadronic energy densities given by Eq. (4.5). This time is roughly the time it takes the compressed nucleus to increase its volume by a factor of 4. For a uranium nucleus, this corresponds to the time it takes a sound wave to travel  $\sim 2.5$  fm, or

$$\tau \sim 4 \text{ fm} \quad . \quad (4.18)$$

The total lifetime of the fireball is  $\sim 8$  fm, a time which is very long compared to the hadronic time scale  $\sim 1$  fm.

Even during the time before the nucleus fireball begins expanding, the fireball constituents scatter many times. During this time the original nucleon constituents of the plasma would scatter  $\sim 30$  times. Mesons would scatter  $\sim 20$  times. Even quarks with their relatively long mean free paths scatter  $\sim 10$  times. This large number of collisions should allow for equipartitioning of the energy. A thorough analysis using relativistic hydrodynamic equations which follow the initial formation and subsequent decay of the fireball should nevertheless be carried out to obtain a precise estimate of the cooling time.

Finally, there is one last problem which we have not touched upon: the uniformity of heat deposition in the nucleus. As the projectile nucleus sweeps through the target, it heats the target primarily by the

inelastic production of pions. These pions materialize primarily on the side of the nucleus which is farthest from the side which faces the incident projectile. This non-uniformity of energy deposition might induce large thermal gradients in the fireball. Such possible thermal gradients should be the subject of further study, since they may allow for the formation of local hot spots within the fireball.

ACKNOWLEDGEMENTS

The authors wish to thank Miklos Gyulassy for his interest and enlightened criticism of this work. We also gratefully acknowledge many useful discussions with Carleton DeTar, Mike Dine, Jack Gunion, Harry Lam, Herbert Ruck, Leo Stodolsky, and M. Weinstein. One of the authors, R. Anishetty, thanks the SLAC Theory Group for their kind hospitality during his visit. Another of the authors, P. Koehler, wishes to thank the SLAC Theory Group for their kind hospitality, and the Deutscher Akademischer Austauschdienst for their support through a NATO Fellowship. The authors also are grateful to Alice McLerran for assisting with the editing of the manuscript. This work was supported by the Department of Energy under contract numbers DE-AC03-76SF00515 (SLAC) and DE-AC06-76ER01388 (Washington).

REFERENCES

1. V. K. Balasubrahmanyam and J. F. Ormes, *Astrophys. J.* 186, 109 (1973).
2. E. Juliusson *et al.*, *Astrophys. J.* 191, 331 (1974).
3. C. D. Orth *et al.*, *Astrophys. J.* 226, 1147 (1978).
4. J. A. Goodman *et al.*, *Phys. Rev. Lett.* 42, 854 (1979), and *Phys. Rev. D* 19, 2572 (1979); J. A. Goodman, Ph.D. Thesis, University of Maryland, UMI 79-08853 (1978) (unpublished).
5. P. S. Freier and C. J. Waddington, in *Cosmic Rays and Particle Physics*, Bartol Conference (1978); T. K. Gaisser, ed., *The American Institute of Physics*, New York (1979); *AIP Conference Proceedings*, No. 49, p. 87.
6. H. E. Bergeson *et al.*, *Phys. Rev. Lett.* 39, 847 (1977).
7. G. Tarlé, P. B. Price and E. K. Shirk, *Proceedings of the 16th International Cosmic Ray Conference*, T3-13 (1979).
8. J. Wilkes *et al.*, *Report of Japanese-American Cooperative Experiment to Measure Composition, Energy Spectra, and Interactions of Cosmic Rays at Energies up to  $10^{14}$  eV* (unpublished).
9. *The Venus Project*, LBL-PUB-5025 (1979) (unpublished).
10. *Numatron-High Energy Heavy-Ion Facility*, University of Tokyo Report (1977).
11. *Eine Beschleunigeranlage für Relativistische Schwere Ionen*, Gesellschaft für Schwerionenforschung mbH Darmstadt (1979).
12. N. Itoh, *Prog. Theor. Phys.* 44, 291 (1970).
13. F. Iachello, W. D. Langer and A. Lande, *Nucl. Phys.* A219, 612 (1974).
14. J. C. Collins and M. J. Perry, *Phys. Rev. Lett.* 34, 1353 (1975).
15. G. Baym and S. A. Chin, *Phys. Lett.* 62B, 241 (1976).

16. G. Chapline and M. Nauenberg, *Nature (Lond.)* 264, 235 (1976).
17. B. A. Freedman and L. L. D. McLerran, MIT Report-541 (1976) (unpublished).
18. M. B. Kislinger and P. D. Morley, *Phys. Rev.* D13, 2771 (1976).
19. B. A. Freedman and L. D. McLerran, *Phys. Rev.* D16, 1130 (1977), D16, 1147 (1977), D16, 1169 (1977), and D17, 1109 (1978).
20. G. Chapline and M. Nauenberg, *Phys. Rev.* D16, 450 (1977).
21. M. B. Kislinger and P. D. Morley, *Phys. Lett.* 67B, 371 (1977).
22. V. Baluni, *Phys. Lett.* 72B, 381 (1978).
23. P. D. Morley, *Phys. Rev.* D17, 598 (1978).
24. V. Baluni, *Phys. Rev.* D17, 2092 (1978).
25. M. B. Kislinger and P. D. Morley, *Astrophys. J.* 219, 1917 (1978).
26. B. J. Harrington and H. K. Shepard, *Nucl. Phys.* B124, 409 (1977), *Phys. Rev.* D17, 2122 (1978), and D18, 2990 (1978).
27. E. V. Shuryak, *Phys. Lett.* 79B, 135 (1978).
28. C. G. Källman, *Phys. Lett.* 85B, 392 (1979).
29. N. Bilić and D. E. Miller, *Phys. Lett.* 87B, 239 (1979), and Bielefeld Preprint BI-TP 80/02 (unpublished).
30. J. I. Kapusta, *Nucl. Phys.* B148, 461 (1979).
31. J. Kuti, B. Lukacs, J. Polonyi and K. Szlachanyi, CERN Preprint TH-2839 (unpublished).
32. H. Satz, "From Hadron to Quark Matter" in *Hadronic Matter at Extreme Energy Density*, Plenum Press, New York and London (1980); F. Karsch and H. Satz, *Phys. Rev.* D21, 1168 (1980), and Bielefeld Preprint BI-TP 80/03 (unpublished).
33. G. 't Hooft, *Nucl. Phys.* B153, 141 (1979).

34. L. Susskind, Phys. Rev. D20, 2610 (1979); A. M. Polyakov, Phys. Lett. 72B, 477 (1978).
35. H. Miyazawa, Phys. Rev. D20, 2953 (1979).
36. G. Lasher, Phys. Rev. Lett. 42, 1646 (1979).
37. G. Steigman and R. V. Wagoner, Phys. Rev. D20, 825 (1979).
38. S. A. Chin, Phys. Lett. 78B, 552 (1978).
39. N. K. Glendenning and Y. J. Karant, LBL Report 8653 (1979) (unpublished).
40. K. A. Olive, Phys. Lett. 89B, 299 (1980).
41. G. Domokos and J. I. Goldman, Johns Hopkins University Preprint HET-8004 (1980) (unpublished).
42. T. K. Gaisser, P. S. Freier and C. J. Waddington, Proceedings of the 16th International Cosmic Ray Conference HEI, 251 (1979).
43. J. A. Goodman et al., Proceedings of the 16th International Cosmic Ray Conference EAI, 37 (1979).
44. M. F. Kaplon, D. M. Ritson and W. D. Walker, Phys. Rev. 90, 716 (1953).
45. E. Lohrmann and M. W. Teucher, Nuovo Cimento 25, 957 (1962), and earlier references therein.
46. E. L. Feinberg, Phys. Rep. 5C, 237 (1972).
47. A. Gurtu et al., Tata Institute Report TIFR-BC-74-6, published in Leipzig Symposium (1974), p. 493, and earlier references therein.
48. P. R. Vishwanath et al., Phys. Lett. 53B, 479 (1975).
49. J. Hébert et al., Phys. Lett. 48B, 467 (1974).
50. J. Babecki et al., Phys. Lett. 47B, 268 (1973).
51. W. Busza et al., Phys. Rev. Lett. 34, 836 (1975); W. Busza, Proceedings of VII Symposium on Multiparticle Dynamics, Tutzing (1976), p. 545.

52. S. Á. Azimov et al., Phys. Lett. B73, 500 (1978).
53. T. Ferbel, Proceedings of the First Workshop on Ultra-Relativistic Nuclear Collisions, Berkeley, California, LBL-8957 (1979), p. 1.
54. L. D. Landau and I. Ya Pomeranchuk, Dokl. Akad. Nauk SSSR [Sov. Phys.-Doklady] 92, 735 (1953).
55. E. L. Feinberg and I. Ya Pomeranchuk, Dokl. Akad. Nauk. SSSR 93, No. 3, pp. 439-441 (1953) in Russian; E. L. Feinberg, Zh. Tekh. Fiz. [Sov. Phys.-Tech. Phys.] 50, 202 (1966).
56. K. Gottfried, Proceedings of the V International Conference on High Energy Physics and Nuclear Structure, Uppsala (1973).
57. O. V. Kancheli, Zh. Eksp. Teor. Fiz. Pis'ma Red. 18, 465 (1973), and Eng. Trans. JETP Lett. 18, 274 (1973).
58. L. Stodolsky, Proceedings of the VI Symposium on Multiparticle Dynamics, Oxford (1975), p. 577; SLAC Preprint PUB-1052 (1972) (unpublished).
59. G. A. Winbow, Proceedings of the VII Symposium on Multiparticle Dynamics, Tutzing (1976), p. 153.
60. N. N. Nikolaev, A. Ya Ostapchuk and V. R. Zoller, CERN Preprint TH-2547 (1978) (unpublished); N. N. Nikolaev, Landau Institute Preprint 1980-5 (1979) (unpublished).
61. A. S. Goldhaber, Phys. Rev. Lett. 35, 748 (1975).
62. J. Bjorken, Lectures at DESY Summer Institute (1975); SLAC Preprint PUB-1756 (1976) (unpublished).
63. A. Bialas, Proceedings of the First Workshop on Ultra-Relativistic Nuclear Collisions (1979), p. 63.
64. S. Das Gupta, Phys. Rev. Lett. 41, 1450 (1978).

65. S. Das Gupta and C. S. Lam, Phys. Rev. C20, 1192 (1979).
66. This picture of nucleus-nucleus scattering is reminiscent of the Flying Fire-sausage picture of hadron-hadron scattering advocated by G. Preparata and G. Valenti, CERN Preprint CERN-EP 80-47 (1980).
67. W. Thomé et al., Nucl. Phys. B129, 365 (1977).
68. P. Capiluppi et al., Nucl. Phys. B79, 189 (1974).
69. D. Amati, A. Stanghellini and S. Fubini, Nuovo Cimento 26, 896 (1962).
70. K. Wilson, Acta Phys. Austriaca, Vol. 17, No. 1 (1963), pp. 37-44.
71. C. DeTar, Phys. Rev. D3, 128 (1971).
72. R. P. Feynman, Phys. Rev. Lett. 23, 1415 (1969); "Photon-Hadron Interactions," W.A. Benjamin, Inc. (1972).
73. S. J. Brodsky, J. F. Gunion and J. H. Kuhn, Phys. Rev. Lett. 39, 1120 (1977); S. J. Brodsky, Proceedings of the First Workshop on Ultra-Relativistic Nuclear Collisions, Berkeley, California, LBL-8957 (1979), p. 419.
74. R. Blankenbecler and S. J. Brodsky, Phys. Rev. D10, 2973 (1974).
75. S. J. Brodsky and J. F. Gunion, Phys. Rev. D17, 848 (1978).

TABLE 1

A Few Typical Nuclear Radii

Nucleus	Radius
H	.8 fm*
Li <sup>3</sup>	1.7 fm
O <sup>16</sup>	3.0 fm
Fe <sup>56</sup>	4.6 fm
Ru <sup>101</sup>	5.6 fm
Pb <sup>208</sup>	7.1 fm
U <sup>238</sup>	7.4 fm

\* This number is the proton r.m.s. radius determined from electron proton scattering.

TABLE 2

Approximate Multiplicities at High Energies

$E_{c.m.}$	$\langle n_{\pi^+} \rangle$	$\langle n_{\pi^-} \rangle$	$\langle n_{\pi^0} \rangle$	$\langle n_{K^+} \rangle$	$\langle n_{K^-} \rangle$	$\langle n_{K^0} \rangle$	$\langle n_{\bar{K}^0} \rangle$	$\langle n_B \rangle$	$\langle n^{ch} \rangle$	$\langle n^{ch} \rangle_{exp}^*$
30.8	3.4	2.7	3.0	.2	.1	.2	.1	2.	8.4	9.5
45.2	4.4	3.7	4.0	.4	.2	.3	.2	2.	10.7	11.0
53.2	4.9	4.2	4.5	.4	.3	.3	.3	2.	11.8	11.8
62.8	5.4	4.7	5.0	.5	.3	.4	.3	2.	12.9	12.7

\* All numbers in this table are estimates based on the fit described in the paper, except for this last column which is taken from Thomé et al.

TABLE 3

The multiplicity/nucleon, energy/nucleon, momentum/nucleon, rest frame energy/nucleon, and  $\gamma$  of the fireball for various values of the parameters  $\lambda$ ,  $f_\pi$ ,  $f_K$ , and  $f_p$ . The values quoted here use  $E_{c.m.} = 50$  GeV/nucleon, and assume an effective pion mass of  $\sim 300$  MeV. The effective kaon mass is taken as 500 MeV and the proton mass is 1 GeV. The multiplicity, energy, and momentum are per nucleon of the initial nucleus. The rest frame energy is per nucleon of the final fireball. The nucleus we consider is uranium.

Species	Number/Nucl.	$p_{\parallel}$ GeV/Nucl.	E GeV/Nucl.	
Nucleons	.93	1.7	2.2	$\lambda = \frac{1}{2}; f_\pi = f_K = f_N = \frac{1}{2}$ $\gamma = 1.6$ $M_{F.B.} = 2.4$ GeV/Nucl.
Pions	2.2	1.2	1.5	
Kaons	.09	.1	.12	
Nucleons	.97	2.2	2.7	$\lambda = \frac{1}{2}; f_i = 1$ $\gamma = 1.7$ $M_{F.B.} = 2.6$ GeV/Nucl.
Pions	2.2	1.3	1.6	
Kaons	.09	.1	.12	
Nucleons	.95	1.8	2.3	$\lambda = 1; f_i = \frac{1}{2}$ $\gamma = 1.9$ $M_{F.B.} = 3.2$ GeV/Nucl.
Pions	3.4	3.0	3.4	
Kaons	.19	.35	.39	
Nucleons	.97	2.4	2.9	$\lambda = 1; f_i = 1$ $\gamma = 2.08$ $M_{F.B.} = 3.6$ GeV/Nucl.
Pions	3.5	3.8	4.2	
Kaons	.2	.4	.43	
Nucleons	.99	2.91	3.4	$\lambda = 1; f_i = 2$ $\gamma = 2.15$ $M_{F.B.} = 3.74$ GeV/Nucl.
Pions	3.53	3.85	4.2	
Kaons	.2	.4	.43	
Nucleons	.98	2.6	3.1	$\lambda = 2; f_i = 1$ $\gamma = 2.74$ $M_{F.B.} = 5.08$ GeV/Nucl.
Pions	4.95	9.1	9.6	
Kaons	.34	1.2	1.2	
Nucleons	.99	3.1	3.6	$\lambda = 2; f_i = 2$ $\gamma = 2.84$ $M_{F.B.} = 5.31$ GeV/Nucl.
Pions	5.0	9.8	10.2	
Kaons	.34	1.2	1.2	

TABLE 4

The parameters and numbers given in this table are determined in the same manner as those of Table 3, except that we consider various center-of-mass energies. The parameters  $\lambda$  and  $f$  are all = 1.

Species	Number/Nucl.	$p_{\parallel}$ GeV/Nucl.	E GeV/Nucl.	
Nucleons	.97	2.4	2.9	$E_{c.m.} = 30$ GeV/Nucl.
Pions	3.0	3.2	3.5	$\gamma = 2.0$
Kaons	.17	.34	.37	$M_{F.B.} = 3.3$ GeV/Nucl.
Nucleons	.97	2.4	2.9	$E_{c.m.} = 50$ GeV/Nucl.
Pions	3.5	3.8	4.2	$\gamma = 2.08$
Kaons	.2	.4	.43	$M_{F.B.} = 3.6$ GeV/Nucl.
Nucleons	.97	2.4	2.9	$E_{c.m.} = 70$ GeV/Nucl.
Pions	3.9	4.2	4.9	$\gamma = 2.1$
Kaons	.21	.44	.47	$M_{F.B.} = 3.8$ GeV/Nucl.

TABLE 5

The parameters and numbers given in this table are determined in the same manner as those of Table 3, except that we consider various nuclear radii. The center-of-mass energy is  $E_{c.m.} = 50$  GeV/nucleon and  $\lambda = f_{\pi} = f_K = f_p = 1$ .

Species	Number/Nucl.	$p_{\parallel}$ GeV/Nucl.	$E$ GeV/Nucl.	
Nucleons	.95	1.9	2.4	$R = 4.6$ fm
Pions	2.6	1.8	2.1	$\gamma = 1.7$
Kaons	.1	.16	.18	$M_{F.B.} = 2.7$ GeV/Nucl.
Nucleons	.96	2.1	2.6	$R = 5.6$ fm
Pions	3.0	2.5	2.8	$\gamma = 1.8$
Kaons	.14	.23	.26	$M_{F.B.} = 3.0$ GeV/Nucl.
Nucleons	.97	2.35	2.85	$R = 7.1$ fm
Pions	3.45	3.6	4.0	$\gamma = 2.0$
Kaons	.19	.37	.4	$M_{F.B.} = 3.5$ GeV/Nucl.
Nucleons	.97	2.4	2.9	$R = 7.4$ fm
Pions	3.5	3.8	4.2	$\gamma = 2.0$
Kaons	.2	.4	.43	$M_{F.B.} = 3.6$ GeV/Nucl.

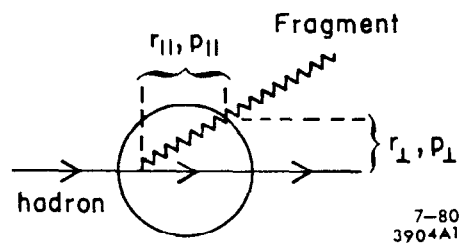


Fig. 1. The formation of a hadron fragment in a hadron-nucleus collision.